O.E.C.D. HIGH TEMPERATURE REACTOR PROJECT

DRAGON

Dragon Project Report

THE COMPARISON OF CARBON-ATOM DISPLACEMENT RATE IN GRAPHITE IN THE DRAGON REACTOR, THE PETTEN HFR AND OTHER REACTORS

by

D.L. REED

A.E.E. Winfrith, Dorchester, Dorset, England

August, 1968

THE COMPARISON OF CARBON-ATOM DISPLACEMENT RATE IN GRAPHITE IN THE DRAGON REACTOR, THE PETTEN HFR AND OTHER REACTORS

by

D. L. REED

ABSTRACT

A revision of the Monte-Carlo calculations in [2] has been made and the ratio of the carbon-atom displacement rate per unit nickel fission flux in the Dragon capsule in Petten to that in the TE.10 hole in BEPO was found to be 0.49 as compared to the experimental value of 0.52. This result together with results reported in [4] for other reactor systems gives us confidence in using the Monte-Carlo method for obtaining the ratio of carbon-atom displacement rate per unit nickel fission flux from one reactor to another. Calculations have therefore been made using this method to relate the carbon-atom displacement rate per unit nickel fission flux in Dragon and a number of proposed HTR's with that in a DIDO Mk.III fuel element. These calculations were then used to give the DIDO nickel dose obtained in Dragon, and the proposed HTR's after a period of 300 days. It was found that the average DIDO nickel dose across a cell of a reactor was proportional to the power density for the reactor systems considered.

CONTENTS

		PAGE NO.
1.	INTRODUCTION	5
2.	PART I - COMPARISON OF CARBON-ATOM DISPLACEMENT RATE IN A NUMBER OF REACTOR SYSTEMS	6
	2.1 Description of the Method	6
	2.2 Comparison of the Monte-Carlo Calculation with Experiment	9
	2.3 Comparison of Carbon-Atom Displacement Rate Between the Centre and Edge Position in the Petten HFR	10
	2.4 Conclusions to Part I	11
3.	PART II - CALCULATION OF THE DIDO NICKEL FLUX AND THE CARBON-ATOM DISPLACEMENT RATES IN HOMOGENEOUS AND HETEROGENEOUS REACTOR SYSTEMS	12
	3.1 The Method of Calculation	12
	3.2 Details of the Calculations	14
	3.3 Results	19
	3.4 Additional Calculations	19
	3.5 Conclusions to Part II	27
4.	REFERENCES	28

LIST OF TABLES

TABLE		
1.	Summary of Results	8
2.	Comparison of Theoretical and Experimental Results	9
3.	Carbon-Atom Displacement Rates	10
4.	Material Densities in the Cell for Case (2a)	15
5.	Material Densities in the Cell for Case (2b)	16
6.	Boundaries of Regions in the Cell for Case (3)	17
7.	Boundaries of Regions in the Cell for Case (4)	17
8.	Boundaries of Regions within Each Fuel Pin	18

TABLE PAGE NO.

9. Material Densities in the Fuel Region of a Fuel Pin 18

10. Results for an Homogeneous HTR with 1.7 g/cm^3 Heavy Metal Loading in the Fuel Region 20

11. Results for an Homogeneous HTR with 1.0 g/cm^3 Heavy Metal Loading 21

12. Results for an Heterogeneous Low Enrichment HTR with a Core Power Density of 8 MW/m^3 22

13. Results for an Heterogeneous Low Enrichment HTR with the Fuel in the Form of a Cluster of 18 Pins 23

14. Length of Time to Irradiate the Fuel of Various Types of HTR's in Dragon to a Given Burn-up 24

15. Comparison of Average DIDO Nickel Dose in a Cell of a Reactor with that Predicted by Assuming that the DIDO Nickel Dose is Proportional to Power Density 25

16. Results for an Homogeneous HTR with 1.0 g/cm^3 Heavy Metal Loading at 5.8 MW/m^3 26

LIST OF ILLUSTRATIONS

FIGURE

1. Neutron Spectra in the Dragon Capsule in Position E8 in Petten HFR

2. Case 1 - Sections through the Dragon Reactor Showing Regions in which Neutron Spectra were Calculated

3. Cases 2a and 2b - Dimensions of the Cell of a Homogeneous HTR and the Regions for which Neutron Spectra were Calculated

4. Case 4 - Regions in which Neutron Spectra were Calculated for the Heterogeneous HTR with the Fuel in the Form of a Cluster of Pins

5. Case 2a - DIDO Nickel Dose after 300 Days Versus Cell Radius

6. Case 2b - DIDO Nickel Dose after 300 Days Versus Cell Radius

7. Case 3 - DIDO Nickel Dose after 300 Days Versus Cell Radius

8. Case 4 - DIDO Nickel Dose after 300 Days Versus Cell Radius

9. Comparison of the DIDO Doses after 300 Days Across a Cell for Two Different Heavy Metal Loadings

FIGURE

10. The Change of DIDO Nickel Dose Profile in a Cell of a Low Enrichment HTR with Increase in Size of the Moderator Region but keeping the Cell Volume Constant

11. Case 2a1 - DIDO Nickel Dose after 300 Days Versus Cell Radius

12. Case 2a2 - DIDO Nickel Dose after 300 Days Versus Cell Radius

THE COMPARISON OF CARBON-ATOM DISPLACEMENT RATE IN GRAPHITE IN THE DRAGON REACTOR, THE PETTEN HFR AND OTHER REACTORS

by

D. L. REED

1. INTRODUCTION

An experiment [1] has now been made to obtain the relationship between the number of carbon-atom displacements per unit nickel flux in the Dragon capsule at core position E8 in the Petten HFR to that in DIDO. The results show that there is an almost one to one relationship. This result is in contradiction to the calculations made using the Monte-Carlo method reported in [2]. A reappraisal of the Monte-Carlo calculations previously carried out has therefore been made and this paper describes these additional calculations and is divided into two parts.

Part I of the paper is concerned with the comparison of the carbon-atom displacement rate between Dragon, the Petten HFR and DIDO. Also a comparison has been made between carbon-atom displacement rates predicted using neutron spectra calculated by diffusion theory and the corresponding Monte-Carlo method. An attempt has also been made to compare the carbon-atom displacement rates for the American GETR with DIDO using neutron spectra calculated by a transport theory code. In addition work has also been carried out using the Monte-Carlo method in conjunction with MUGDI calculations by W. Zijp [3], to compare carbon-atom displacement rates in a Dragon capsule placed at the edge and the centre of the Petten HFR core.

Part II gives the results of calculations concerning the carbon-atom displacement rates in proposed HTR's. Five cases have been considered, these are:

(1) Dragon with a power density of 14 MW/m^3.

(2a) An homogeneous low enrichment HTR with 1.7 g/cm^2 heavy metal loading.

(2b) An homogeneous low enrichment HTR with 1.0 g/cm^2 heavy metal loading.

(3) An heterogeneous low enrichment HTR described in Part II of [2].

(4) An heterogeneous low enrichment HTR with the fuel in the form of a cluster of 18 pins.

In addition three further points were investigated:

(a) the effect of increasing the voidage in an homogeneous HTR,

(b) the change in fine structure of the nickel flux across a cell of an homogeneous HTR as a result of changing the fuel heavy metal loading density, and

(c) the change in fine structure of the nickel flux across a cell of an heterogeneous HTR as a result of reducing the size of the fuel region but keeping the cell volume the same.

Each of these cases will be described in turn in Part II of the paper.

2. PART I - COMPARISON OF CARBON-ATOM DISPLACEMENT RATE IN A NUMBER OF REACTOR SYSTEMS

2.1 Description of the Method

A complete description of the method of calculation has been given in [2] but some of the symbols used are given here to enable the results to be followed more easily:

$$\bar{D} = \frac{\int_{0.01}^{10\ \text{MeV}} \sigma_s \, d\phi \, dE}{\int_{0.01}^{10\ \text{MeV}} \phi \, dE} = \text{the average number of carbon-atom displacements in graphite}$$

$$\bar{\sigma}_{Ni} = \frac{\int_{0.01}^{10\ \text{MeV}} \sigma_{Ni}\,(n,p)\,\phi \, dE}{\int_{0.01}^{10\ \text{MeV}} \phi \, dE}$$

$$\bar{\sigma}_{Fe} = \frac{\int_{0.01}^{10\ \text{MeV}} \sigma_{Fe}\,(n,p)\,\phi \, dE}{\int_{0.01}^{10\ \text{MeV}} \phi \, dE}$$

where:

σ_s = carbon scattering cross section

d = number of carbon-atom displacement in graphite

$\phi \, dE$ = neutron flux between energies E and E + dE

σ_{Ni} (n,p) = Ni-58 (n,p) Co-58 cross section

σ_{Fe} (n,p) = Fe-54 (n,p) cross section

The corresponding average number of carbon-atom displacements and cross sections with a primary fission spectrum are:

$\hat{D}$, $\hat{\sigma}_{Ni}$, $\hat{\sigma}_{Fe}$

In order to compare the number of carbon-atom displacements per unit flux from one reactor to another the quantity $\bar{D}\frac{\hat{\sigma}_{Ni}}{\bar{\sigma}_{Ni}}$ was calculated, which is the number of carbon-atom displacements per unit nickel flux. A summary of the results is given in Table 1, where $\hat{\sigma}_{Ni}$ = 107 mb, $\hat{\sigma}_{Fe}$ = 77 mb and $\bar{D}$ was calculated using the Thompson-Wright Model for carbon damage [4].

The last column in Table 1 gives the ratio of the equivalent nickel flux in DIDO ϕ_{DIDO} (Ni), (i.e., that nickel flux in DIDO which gives the same carbon-atom displacement rate as in the irradiation facility) to the total neutron flux above 0.18 MeV, ϕ (>0.18 MeV).

The results of particular interest in Table 1 are the comparison of the CRAM and Monte-Carlo calculations for the calibration experiment in a Dragon capsule in the Petten HFR. Fig. 1 compares the spectra from the two calculations which have been normalised over the entire energy range above 0.01 MeV and shows that they are in reasonable agreement everywhere except above 1 MeV. From Table 1 it is seen that $\bar{D}$, $\bar{\sigma}_{Ni}$, $\bar{\sigma}_{Fe}$ differ by 6%, 30% and 33% respectively between the two methods of calculation. These differences may be due to the coarse group structure of the CRAM spectrum especially for the energies above 1 MeV where ϕ, σ_{Ni}, σ_{Fe} change rapidly with energy. Again, a further contribution to these differences may be due to the way in which the cross section data have been condensed for each energy group in the CRAM spectrum, this was done using a linear interpolation method. Finally the last contribution is due to CRAM producing a spectrum which differs from the Monte-Carlo spectrum above 1 MeV. From these considerations it is clear that the calculations of carbon-atom displacement rate per unit nickel dose using CRAM is less reliable than that obtained by the Monte-Carlo method where good agreement with experiment is obtained.

Included in Table 1 are results from calculations based on the neutron spectra obtained for the GETR [6] where a large number of graphite irradiation have been carried out by a number of groups in the U.S.A. These calculations are useful in relating the dose scale used in these irradiations to the equivalent DIDO nickel dose scale. Since the group structure of these spectra are the same as those used in CRAM there is a possibility that the values of $\bar{\sigma}_{Ni}$, $\bar{\sigma}_{Fe}$ and hence

Table 1

Summary of Results

Irradiation Facility	Method of Calculation	$\bar{D}$	$\bar{\sigma}_{Ni}$ mb	$\bar{\sigma}_{Fe}$ mb	$\bar{D}\frac{\hat{\sigma}_{Ni}}{\bar{\sigma}_{Ni}}$	$\frac{\phi_{DIDO}\ (Ni)}{\phi\ (>0.18\ MeV)}$
TE.10 Experimental Hole in BEPO	Monte-Carlo (4)				3,037	
PLUTO Hollow Fuel Element	Monte-Carlo (4)				1,313	
PLUTO Empty Lattice Position	Monte-Carlo (4)				1,299	
Petten HFR Position E.8 (Calibration Capsule)	CRAM (5)	604.2	53.4	34.5	1,212	0.68
Petten HFR Position E.8 (Calibration Capsule)	Monte-Carlo	509.5	41.0	25.9	1,485	0.60
Dragon (First Core)	Monte-Carlo	520.2	25.7	15.7	2,168	0.66
Battelle GETR (Position E.7)	Transport Theory (2 DXY Code) (6)	542.5	38.9	25.1	1,975	0.66
Battelle GETR (Position D.7)	Transport Theory (2 DXY Code) (6)	530.6	32.8	21.2	1,732	0.67
Battelle GETR (6 x Basket)	Transport Theory (2 DXY Code) (6)	552.2	45.0	29.2	1,313	0.65

(4) Calculations by S. B. Wright [4].

(5) Calculations by W. Zijp [5].

(6) Calculations by Yoshikawa [6].

$\bar{D}\frac{\hat{\sigma}_{Ni}}{\bar{\sigma}_{Ni}}$ are in error. Unfortunately a Monte-Carlo calculation has not been carried out to check this point. In addition it was assumed that the spectra had a $\frac{1}{E}$ dependence between 0.18 MeV and 0.01 MeV.

Finally a Monte-Carlo calculation with revised data has been carried out for the central region of the first Dragon core and the results are given in Table 1. The value of carbon-atom displacement rate per unit nickel dose differs by 11% from that previously calculated in [2]. Since the statistical errors of both calculations are each 10% this difference is not very significant.

2.2 Comparison of the Monte-Carlo Calculation with Experiment

In Table 2 a comparison is made between the experimental and Monte-Carlo values of carbon-atom displacement per unit nickel flux normalised to 1.0 at the TE.10 position in BEPO.

Table 2

Comparison of Theoretical and Experimental Results

Irradiation Position	Theory	Experiment
TE.10 Experimental Hole in BEPO	1.0	1.0
PLUTO Hollow Fuel Element	0.43	0.49 (7) 0.48 (8)
PLUTO Replaced Fuel Element	0.43	0.59 (7) 0.51 (8)
Petten HFR Position E.8 Calibration Experiment	0.49	0.52

(7) Bell, et al. - 1962 [7].

(8) Gray - 1964 [8].

For the calibration experiment in the Petten HFR a fuel element in E.8 was replaced by the Dragon capsule consisting of a cylinder of graphite contained in a stainless steel tube. Hence the result in Petten should be compared with the replaced fuel element result in PLUTO. From Table 2 it is seen that good agreement is obtained between the experiments in PLUTO and Petten and also that the Monte-Carlo calculations for Petten are in better agreement with experiment than that for the Empty Lattice position in PLUTO.

2.3 Comparison of Carbon-Atom Displacement Rate Between the Centre and Edge Position in the Petten HFR

The object of this work was to find what would happen to the graphite damage rate in the Dragon capsule if it was moved from the edge to the centre of the Petten HFR. To do this two types of calculations were carried out:

(1) MUGDI (a four group diffusion code) calculations to give the ratio of the nickel flux or the carbon damage flux from one position to another.

(2) Monte-Carlo calculations to give the number of carbon-atom displacements per unit flux in the two cases. These particular Monte-Carlo calculations were made with a lower threshold of 0.0674 MeV since the two high energy groups of interest in MUGDI have thresholds of 1.35 MeV and 0.0674 MeV respectively. The flux ϕ_1 with $E \geq 1.35$ MeV was taken to be proportional to the nickel flux and the flux $(\phi_1 + \phi_2)$ with $E \geq 0.0674$ MeV was taken to be proportional to the graphite damage flux. Two core loadings were considered:

   (a) Core 10300, with the Dragon capsule in position E.8, i.e., at the edge of the core.

   (b) Core 30300, with the Dragon capsule in position E.5, i.e., in the central region of the core.

The results of the calculations are given in Table 3 where the carbon-atom displacement rate was calculated using the Thompson-Wright model and $\hat{\sigma}_{Ni} = 107$ mb.

Table 3

Carbon-Atom Displacement Rates

Core	$\bar{D}$	$\bar{\sigma}_{Ni}$ mb	$\bar{D}\frac{\hat{\sigma}_{Ni}}{\bar{\sigma}_{Ni}}$	ϕ_1	$\phi_1 + \phi_2$
10300	679.3	56.8	1,279	0.432	1.155
30300	682.4	63.6	1,148	0.784	2.035

If it is assumed that the carbon-atom displacement rate:

$$D \propto \bar{D} \, (\phi_1 + \phi_2)$$

then

$$\frac{D_{30300}}{D_{10300}} = 1.77$$

Alternatively if it is assumed that ϕ_1 is proportioned to the nickel flux then:

$$D \propto \bar{D} \, \frac{\hat{\sigma}_{Ni}}{\bar{\sigma}_{Ni}} \, \phi_1$$

so that

$$\frac{D_{30300}}{D_{10300}} = 1.63$$

The error in the estimation of $\bar{D}$ and $\bar{\sigma}_{Ni}$ are 3% and 11% respectively so that the two calculations of $\frac{D_{30300}}{D_{10300}}$ essentially give the same values since they differ by 8.6%, the average being 1.7. The important conclusion from the calculations is that the number of carbon-atom displacement per unit nickel flux does not change significantly in the Dragon capsule if it is moved from the edge to the centre of the core. Hence the change in carbon-atom displacement rate is determined only by the enhancement of the flux from one position to another in the core.

2.4 Conclusions to Part I

After a revision of the input data in the Monte-Carlo calculations reported in [2] good agreement was obtained between the carbon-atom displacement rate per unit nickel flux predicted by the calculations and that obtained in the calibration experiment in the Petten HFR. The calculations based on a CRAM spectrum are not in such good agreement with the experiment and this is possibly due to:

(a) The course group structure of the spectrum.

(b) The method used to obtain the group cross sections, particularly for the iron and nickel (n,p) cross sections.

(c) The fact that CRAM is a diffusion theory code.

These factors lead to quite large discrepancies of the order of 30% between the average nickel and iron (n,p) cross sections predicted by CRAM and the Monte-Carlo method.

The revision in the data for the Monte-Carlo calculations made for the Dragon first core leads to a change of only 11% in the number of carbon-atom displacement per unit nickel dose from the result given in [2].

The carbon-atom displacement rate per unit nickel dose in the Dragon capsule placed at the centre and edge position in the Petten HFR is the same within the errors of the calculations. This leads to an enhancement of the carbon-atom displacement rate of 1.7 if the capsule is moved from the core edge to the centre of the reactor.

The ratio of the equivalent DIDO nickel flux to the total neutron flux above 0.18 MeV $\left(\frac{\phi_{Ni,DIDO}}{\phi(>0.18\ MeV)}\right)$ is on average 0.66 for the GETR. This ratio appears to be almost constant for the reactor systems considered (see Table 1) and it would be of interest to see if this was so for other reactor systems like BEPO and the AGR.

3. PART II - CALCULATION OF THE DIDO NICKEL FLUX AND THE CARBON-ATOM DISPLACEMENT RATES IN HOMOGENEOUS AND HETEROGENEOUS REACTOR SYSTEMS

The purpose of this section of the paper is to compare the DIDO nickel doses achieved in proposed heterogeneous and homogeneous HTR designs and to obtain the time needed to test the fuel to the maximum expected DIDO dose in Dragon. Five cases have been considered, these are:

(1) Dragon with a power density of 14 MW/m^3.

(2a) An homogeneous low enrichment HTR 1.7 g/cm^3 heavy metal loading.

(2b) An homogeneous low enrichment HTR 1 g/cm^3 heavy metal loading.

(3) An heterogeneous low enrichment HTR described in Part II of [2].

(4) An heterogeneous low enrichment HTR with the fuel in the form of a cluster of 18 pins.

Each of these cases will be described in turn in the next part of the paper.

3.1 The Method of Calculation

Except for Dragon only a single cell of the reactor was considered and the neutrons were reflected back into the walls of the cell to take account of the neighbouring cells in the reactor. The source of fast neutrons was considered to be uniform throughout the fuel region. In order to reduce the length of time of the computer calculations the reactor was divided into two parts at the central plane and the neutrons were reflected at this boundary to take account of those neutrons in the other half of the reactor. The cell was then divided into a number of radial regions and axial regions. A total of 10,000 neutrons were

tracked in the cell to below 0.01 MeV and neutron spectra were calculated in every region in the cell. In the case of the homogeneous HTR's the neutron spectra were divided up into 70 equal lethargy groups between 0.01 and 14 MeV and for the heterogeneous cases 20 equal lethargy groups between 1 and 14 MeV and also between 0.01 and 1 MeV.

Using these spectra the programme calculated the Ni-58 (n,p) Co-58 reaction rate and the carbon-atom displacement rate in graphite with the Thompson-Wright model for each region.

From these results the equivalent nickel fission flux per source neutron $\phi_{Ni,fission}$ defined by Equation (1) below was calculated for each region:

$$\phi_{Ni,fission} = \frac{\int_{0.01}^{14\ MeV} \phi\, \sigma_{Ni}\, dE}{S\, \hat{\sigma}_{Ni}} \qquad (1)$$

where:

S = total number of source neutrons in the reactor cell

σ_{Ni} = Ni-58 (n,p) Co-58 cross section for nickel

$\hat{\sigma}_{Ni}$ = 107 mb = average nickel cross section in a primary fission spectrum.

A further correction was applied to the nickel fluxes in order to convert them to the DIDO scale and this correction factor is given in Equation (2):

$$\phi_{Ni,DIDO} = \frac{\bar{\sigma}_D \frac{\hat{\sigma}_{Ni}}{\bar{\sigma}_{Ni}}}{\left[\bar{\sigma}_D \frac{\hat{\sigma}_{Ni}}{\bar{\sigma}_{Ni}}\right]_{DIDO}} \phi_{Ni,fission} \qquad (2)$$

where:

$\bar{\sigma}_D \frac{\hat{\sigma}_{Ni}}{\bar{\sigma}_{Ni}}$ = carbon-atom displacement rate per unit nickel flux in any region

$\bar{\sigma}_D \frac{\hat{\sigma}_{Ni}}{\bar{\sigma}_{Ni}}$ = 1,313 = carbon-atom displacement rate per unit nickel flux in a DIDO hollow fuel element.

A more direct way to calculate $\phi_{Ni,DIDO}$ was actually used since Equations (1) and (2) can be combined to give:

$$\phi_{Ni,DIDO} = \frac{1}{S} \frac{\int_{0.01}^{14\ MeV} \sigma_s\ d\ \phi\ dE}{1313} \qquad (3)$$

The total number of source neutrons in the cell was calculated when the reactor was at a given power and the corresponding fission fluxes in each region were obtained by multiplying Equation (3) by this number.

3.2 Details of the Calculations

Case (1) - Dragon

Here calculations of spectra were carried out in the central thorium region in the core of the Dragon First Charge. Fig. 2 shows the regions in this part of the reactor for which spectra were calculated. The core materials were homogenised and the isotopic number densities used in each region are given in Table A1.8 and A1.9 of [9]. In this calculation the fission source fractions for the regions were deduced from thermal flux measurements [10].

Case (2a) - An Homogeneous Low Enrichment HTR

This case is based on the proposal in [11] for the optimum engineering reference design, i.e., core power density of 5.8 MW/m^3, fuel power density of 46 MW/te, 5% enrichment and 1.7 g/cm^3 heavy metal loading. Fig. 3 shows the regions for which neutron spectra were calculated. In Table 4 the details are given of the isotopic number densities used in each region together with the radii of the regions.

Case (2b)

This is very similar to Case (2a) the difference being that the heavy metal loading in the fuel region was 1 g/cm^3. The core power density was 5.6 MW/m^3, fuel power density 52 MW/te, and fuelled with 5% enrichment uranium. Table 5 gives the material densities in the regions in the cell together with the radii of the regions. The dimensions of the cell are the same as in Fig. 3 except for the outer dimensions.

Case (3) - An Heterogeneous Low Enrichment HTR

This calculation is a repeat of the case given in [2] with the cell divided up into a greater number of radial regions, particularly in the fuel region. The boundaries of the region for which spectrum calculations have been made are given in Table 6.

Table 4

Material Densities in the Cell for Case (2a)

Regions	Radii cm		Number Densities atoms/cm^3 x 10^{24}				Density g/cm^3
	Inner	Outer	Carbon	Oxygen	U-235	U-238	
1, 7, 13	0	1.0	← Void →				0
2, 8, 14	1.0	1.3	0.090375	-	-	-	1.8
3, 9, 15	1.3	2.0	0.02008	0.008614	0.00021792	0.00408839	2.3288
4, 10, 16	2.0	2.566	0.090375	-	-	-	1.8
5, 11, 17	2.566	2.939	← Void →				0
6, 12, 18	2.939	9.907*	0.08032	-	-	-	1.6

*Length of side of outer square boundary of cell.

T

Table 5

Material Densities in the Cell for Case (2b)

Regions	Radii cm		Number Densities atoms/cm^3 x 10^{24}				Density g/cm^3
	Inner	Outer	Carbon	Oxygen	U-235	U-238	
1, 7, 13	0	1.0	← Void →				0
2, 8, 14	1.0	1.3	0.090375	-	-	-	1.8
3, 9, 15	1.3	2.0	0.02811	0.00506624	0.00012819	0.00240493	1.6946
4, 10, 16	2.0	2.566	0.090375	-	-	-	1.8
5, 11, 17	2.566	2.939	← Void →				0
16, 12, 18	2.939	8.231*	0.08032	-	-	-	1.6

*Length of side of the outer square boundary of cell.

Table 6

Boundaries of Regions in the Cell for Case (3)

Radius	cm	2.1	4.0	6.0	8.0	10.0	11.0	12.0	13.2
		13.5	14.0	15.0	16.0	17.0	18.0	19.0	20.0
		21	44*						
Axial height above the central plane of the core	cm	25	50	200					

*Length of side of outer square boundary of cell.

Table 7

Boundaries of Regions in the Cell for Case (4)

Radius	cm	1.75	2.4	7.625	12.75	13.15	13.65	14.45	16.45
		17.0	18.0	19.0	20.00	21.00	22.00	48.95*	
Height above the core central plane	cm	25	50	275					

*Length of side of square cell.

Case (4) - An Heterogeneous Low Enrichment HTR with the Fuel in the Form of a Cluster of 18 Pins

This case is based on an actual heterogeneous HTR design with the fuel at an average power of 50 MW/te. Calculations of spectra were made in 15 concentric radial regions in a square cell of side 48.95 cm. The overall height of the core was taken to be 550 cm. Details of the boundaries of the regions in which spectra were calculated are given in Table 7.

There are six fuel pins in radial region 3 and 12 fuel pins in radial region 4 as shown in Fig. 4. The relative power ratings of the inner and outer rings of fuel pins are 0.92 and 1.04 respectively. Each fuel pin has four material regions and spectra were calculated in these regions the boundaries of which are given below in Table 8.

Table 8

Boundaries of Regions within Each Fuel Pin

Radius	cm	1.15	1.45	2.1	2.456
Height above the core central plane	cm	25	50	275	

The structural graphite in the cell has a density of 1.8 g/cm^3, these are regions 2, 5, 7, and 9 to 15, and also regions 47 and 49 in the fuel pins. Regions 1, 6 and 8 are voids and so is region 46 inside the fuel pin, also the regions in 3 and 4 surrounding the fuel pins are voids. Table 9 below gives the isotopic number densities for the fuel regions in the fuel pins.

Table 9

Material Densities in the Fuel Region of a Fuel Pin

	atoms/barn
Carbon*	0.048116
U-235	0.00021786
U-238	0.0040872
Oxygen	0.0086057
Density g/cm^3	2.8872

*The carbon included the silicon since cross sections for silicon were not available on the data tape.

3.3 Results

For all the cases except Dragon only calculations of $\bar{\sigma}_D \frac{\hat{\sigma}_{Ni}}{\bar{\sigma}_{Ni}}$, $\phi_{Ni,fission}$, $\phi_{Ni,DIDO}$ and the corresponding DIDO nickel dose after 300 days at power are given in Tables 10, 11, 12 and 13 for all radial regions between 0 cm and 25 cm above the central plane of the reactor core. Also Figs. 5, 6, 7 and 8 show the dose after 300 days as a function of radius from the centre of the cell. In the case of Dragon only results for the central region 5 shown in Fig. 2 are given below:

Dragon Core Power Density	= 14	MW/m^3
Nickel Fission Flux ϕ_{Ni} at the centre of the core	= 3.56×10^{13}	$n/cm^2/s$
Equivalent DIDO Nickel Flux $\phi_{Ni,DIDO}$	= 5.88×10^{13}	$n/cm^2/s$
$\bar{\sigma}_D \frac{\hat{\sigma}_{Ni}}{\bar{\sigma}_{Ni}}$	= 2,168	
Equivalent DIDO Nickel Dose after 300 days	= 1.524×10^{21}	n/cm^2

Since some of these fuels for the low enrichment HTR's are being tested in Dragon the length of time required to achieve a fast neutron dose associated with burn-ups of 30,000, 50,000 and 70,000 MWD/te is given in Table 14.

In Table 14 the power densities given are the average for the core. The residence times in Dragon to achieve a fast neutron dose associated with given burn-ups is constant and independent of the fuel power density.

3.4 Additional Calculations

3.4.1 The affect on the carbon-atom displacement rate per unit nickel dose by increasing the voidage in an homogeneous HTR was found for case (1). The voidage in the Dragon core was increased by 35% and the carbon-atom displacement rate per unit nickel dose at the centre of the core changed from 2,168 to 1,975, i.e., a change of 10%. The statistical errors in these displacement rates are the order of 5% so that the difference is the order of two standard deviations which is therefore insignificant.

3.4.2 The change in fine structure of the nickel flux across a cell of an homogeneous HTR as a result of changing the fuel heavy metal loading density was found by decreasing the heavy metal loading in case (2a) from 1.7 g/cm^3 to 1 g/cm^3. The results are given in Table 16 and Fig. 9 and show a negligible change in the fine structure within the statistical errors of the calculation which are of the order of 4%.

T

Table 10 - Case (2a)

Results for an Homogeneous HTR with 1.7 g/cm^3 Heavy Metal Loading in the Fuel Region

Region	Radii cm		Nickel Flux/Source Neutron x 10^3	$\bar{\sigma}_D \frac{\hat{\sigma}_{Ni}}{\bar{\sigma}_{Ni}}$	$\phi_{Ni,DIDO}$ at 46 MW/te x 10^{-13}	DIDO Dose after 300 Days x 10^{-20}
	Inner	Outer				
1	0	1.0	1.9648	1,859	2.3524	6.0974
2	1.0	1.3	1.9535	1,897	2.3869	6.1868
3	1.3	2.0	2.1287	1,824	2.5014	6.4836
4	2.0	2.57	1.7451	2,037	2.2891	5.9333
5	2.57	2.94	1.6500	2,042	2.1698	5.6241
6	2.94	5.591	1.3116	2,411	2.0369	5.2796

T

Table 11 - Case (2b)

Results for an Homogeneous HTR with 1.0 g/cm^3 Heavy Metal Loading

Region	Radii cm		Nickel Flux/Source Neutron x 10^3	$\bar{\sigma}_D \frac{\hat{\sigma}_{Ni}}{\bar{\sigma}_{Ni}}$	$\phi_{Ni,DIDO}$ at 52 MW/te x 10^{-13}	DIDO Dose after 300 Days x 10^{-20}
	Inner	Outer				
1	0	1.0	2.2666	2,330	2.2680	5.8786
2	1.0	1.3	2.4075	2,258	2.3339	6.0495
3	1.3	2.0	2.5204	2,160	2.3380	6.0601
4	2.0	2.57	2.1301	2,425	2.2177	5.7483
5	2.57	2.94	1.9729	2,570	2.1768	5.6423
6	2.94	4.643	1.8137	2,704	2.1055	5.4574

Table 12 - Case (3)

Results for an Heterogeneous Low Enrichment HTR with a Core Power Density of 8 MW/m^3

Region	Radii cm		Nickel Flux/ Source Neutron x 10^4	$\bar{\sigma}_D \frac{\hat{\sigma}_{Ni}}{\bar{\sigma}_{Ni}}$	$\phi_{Ni,DIDO}$ at 46.73 MW/te x 10^{-13}	DIDO Dose after 300 Days x 10^{-20}
	Inner	Outer				
1	0	2.1	1.7729	1,792	5.7168	14.818
2	2.1	4.0	1.7748	1,756	5.6096	14.540
3	4.0	6.0	1.6710	1,861	5.5953	14.503
4	6.0	8.0	1.4272	2,135	5.4842	14.215
5	8.0	10.0	1.6038	1,772	5.1153	13.259
6	10.0	11.0	1.5414	1,693	4.6975	12.176
7	11.0	12.0	1.3681	1,802	4.4363	11.499
8	12.0	13.2	1.0905	2,088	4.0980	10.622
9	13.2	13.5	1.0562	1,931	3.6705	9.5139
10	13.5	14.0	1.0149	1,947	3.5572	9.2202
11	14.0	15.0	0.8123	2,326	3.3996	8.8119
12	15.0	16.0	0.7302	2,342	3.0774	7.9766
13	16.0	17.0	0.5908	2,676	2.8455	7.3757
14	17.0	18.0	0.4810	3,008	2.6034	6.7480
15	18.0	19.0	0.4492	2,950	2.3850	6.1821
16	19.0	20.0	0.4308	2,912	2.2581	5.8531
17	20.0	21.0	0.3875	2,103	2.1641	5.6095
18	21.0	24.89	0.3349	2,922	1.7613	4.5652

Table 13 - Case (4)

Results for an Heterogeneous Low Enrichment HTR with the Fuel in the Form of a Cluster of 16 Pins

Region	Radii cm		Nickel Flux/Source Neutron x 10^{4}	$-\frac{\hat{\sigma}_{Ni}}{\bar{\sigma}_{Ni}}$	$\phi_{Ni,DIDO}$ at 50 MW/te x 10^{-13}	DIDO Nickel Dose after 300 Days x 10^{-20}
	Inner	Outer				
1	0	1.75	1.1634	1,669	3.8261	9.9174
2	1.75	2.4	1.1590	1,823	3.7163	9.6379
5	12.75	13.15	0.7275	2,012	2.5755	6.6757
6	13.15	13.65	0.6914	2,096	2.5504	6.6106
7	13.65	14.45	0.6289	2,146	2.3757	6.1577
8	14.45	16.45	0.5171	2,440	2.2206	5.7558
9	16.45	17.0	0.4810	2,561	2.1679	5.6193
10	17.0	18.0	0.4190	2,639	1.9458	5.0435
11	18.0	19.0	0.3637	2,743	1.7557	4.5508
12	19.0	20.0	0.3174	2,869	1.6025	4.1538
13	20.0	21.0	0.3230	2,680	1,5473	4.0106
14	21.0	22.0	0.3044	2,745	1,4705	3.8116
15	22.0	27.6	0.2322	2,810	1.1481	2.9759
Results for Inner Ring of Fuel Rods - Radial Measurements from the Centre of the Fuel Rod						
46	0	1.15	1.2809	1,640	3.6973	9.5833
47	1.15	1.45	1.3121	1,633	3.7718	9.7765
48	1.45	2.1	1.3372	1,566	3.6813	9.5420
49	2.1	2.456	1.243	1,610	3.5219	9.1285
Results for Outer Ring of Fuel Rods - Radial Measurements from the Centre of the Fuel Rod						
70	0	1.15	1.3143	1,366	3.1804	8.191
71	1.15	1.45	1.3574	1,[illegible]64	3.1846	[illegible]
72	1.45	2.1	1.2102	1,[illegible]37	[illegible]	[illegible]
73	2.1	2.456	[illegible]	1,[illegible]	[illegible]	[illegible]

T

Table 14

Length of Time to Irradiate the Fuel of Various Types of HTR's in Dragon to a Given Burn-up

Case No.	Type of Reactor	Average Core Power Density MW/m^3	Average Fuel Power Density MW/te	DIDO Nickel Dose after 300 Days in the Fuel	Irradiation Time in Dragon in Days to Achieve a Fast Neutron Dose Associated with a Burn-up of:		
					30,000 MWD/te	50,000 MWD/te	70,000 MWD/te
2a	Homogeneous HTR	5.8	46	6.48×10^{20}	277	462	647
2b	Homogeneous HTR	5.6	52	6.06×10^{20}	245	409	573
3	Heterogeneous HTR	8	46.73	1.28×10^{21} (3)	539	899	1,259
4	Heterogeneous HTR	4.6	50	9.54×10^{20} (1)	376	626	876
		4.6	50	8.44×10^{20} (2)	332	554	776

(1) Average DIDO nickel dose in the fuel regions of the inner six fuel pins.

(2) Average DIDO nickel dose in the fuel regions of the outer six fuel pins.

(3) Average DIDO nickel dose in the fuel region.

T

Table 15

Comparison of Average DIDO Nickel Dose in a Cell of a Reactor with that Predicted by Assuming that the DIDO Nickel Dose is Proportional to Power Density

Case No.	Type of Reactor	Fuel Power Density MW/te	Core Power Density MW/m^3	Average DIDO Nickel Dose after 300 Days	Average DIDO Nickel Dose after 300 Days Using Dragon as a Reference
1	Dragon (Region 5)		14	1.524×10^{21}	1.524×10^{21}
2a	Homogeneous HTR	46	5.8	5.436×10^{20}	6.313×10^{20}
2b	Homogeneous HTR	52	5.6	5.613×10^{20}	6.096×10^{20}
3	Heterogeneous HTR	46.73	8	7.95×10^{20}	8.708×10^{20}
4	Heterogeneous HTR	50	4.6	4.87×10^{20}	5.00×10^{20}
2a1	Homogeneous HTR	46	4.2	3.67×10^{20}	4.57×10^{20}
2a2	Homogeneous HTR	46	2.53	2.31×10^{20}	2.75×10^{20}

T

Table 16

Results for an Homogeneous HTR with 1.0 g/cm^3 Heavy Metal Loading at 5.8 MW/m^3

Region	Radii cm		Nickel Flux/Source Neutron x 10^3	$\bar{\sigma}_D \frac{\hat{\sigma}_{Ni}}{\bar{\sigma}_{Ni}}$	$\phi_{Ni,DIDO}$ at 78.2 MW/te x 10^{-13}	DIDO Dose after 300 Days x 10^{-20}
	Inner	Outer				
1	0	1.0	2.8406	2,033	2.4021	6.2262
2	1.0	1.3	2.8679	1,913	2.4252	6.2861
3	1.3	2.0	2.9703	1,756	2.5118	6.5106
4	2.0	2.57	2.7060	2,164	2.2883	5.9313
5	2.57	2.94	2.5996	2,407	2.1983	5.6980
6	2.94	5.591	2.4388	2,634	2.0623	5.3455

3.4.3 The change in fine structure of the nickel flux across a cell of an heterogeneous HTR as a result of reducing the size of the fuel region but keeping the cell volume the same has been carried out using case(3). Here the outer diameter of the fuel region was reduced from 13.2 cm to 10 cm keeping the same amount of fuel in the reduced volume. The space left by reducing the size of the fuel region was filled with graphite with the same density as the moderator. The results are compared with case (3) in Fig. 10. From Fig. 10 it is clear that the nickel dose is reduced by 14% at a radius of 13.2 cm. This decrease of nickel dose in the moderator is accompanied by an increase of 13% at the central region of the fuel. Hence by inserting a removable graphite sleeve between the fined moderator and the fuel a reduction in the nickel dose can be made in the fixed moderator at the expense of increasing the nickel dose in the fuel if the overall power density in the system is required to be the same.

Further the average DIDO nickel dose across the cell is reduced from 7.95 to 6.65 x 10^{20} after 300 days. This shows that the effect of introducing a greater thickness of graphite in the cell volume is to increase the moderating power of the system and that the nickel flux is then not proportional to the power density.

3.4.4 A further check on the proportionality of DIDO nickel dose with power density for the homogeneous reactor systems was carried out by increasing the size of the cell of case (2a). Two cases were considered, these are (2a1) and (2a2) which had cell radii of 6.584 cm and 8.463 cm respectively. The DIDO nickel dose profiles across the cells of these two cases are shown in Figs. 11 and 12.

3.5 Conclusions to Part II

The average DIDO nickel dose over the entire width of the cell for each case has been calculated and compared with the corresponding doses based on the core power density using Dragon as a reference. These results are given in Table 15 and show reasonable agreement with one another.

It is therefore clear that as a guide to the expected average DIDO nickel dose in any other power reactor, all that is needed is to scale the results given in the last column of Table 15 by the ratios of the average core power densities of the respective systems. If however the moderator region is increased beyond that of the systems considered then one finds that the DIDO flux is not proportional to the power density.

A further check on the Monte-Carlo calculation was to compare the calculated with the measured nickel fluxes in Dragon these are 3.56 x 10^{13} and 3 x 10^{13} respectively and are in quite good agreement. To obtain

better agreement between the theoretical and experimental fluxes requires a detailed knowledge of the power profile in the reactor which has not been used in the calculations.

The differences between the DIDO nickel dose profiles across the cell of the heterogeneous and homogeneous reactors shown in Figs. 8, 9, 10 and 11 are clearly seen. For the homogeneous system the fast dose profile is flatter than the heterogeneous system as would be expected and the ratio of the maximum to the minimum fast dose for the former is between 1.1 and 1.2 as against 3.25 to 3.32 for the latter system.

A most important consequence of this work is the calculation of the DIDO nickel dose expected in order to achieve a given burn-up and hence the irradiation time needed to achieve this dose in Dragon. These times have been calculated for three burn-ups and are given in Table 14. The two most important cases to compare are (2a) and (4), these being recommended HTR designs. It is clear that of the two the fuel of the homogeneous system needs less irradiation time in Dragon to achieve the required maximum dose, e.g., 647 as against 876 days for the heterogeneous system corresponding to a burn-up of 70,000 MWD/te.

From the additional calculations it can be concluded that:

(a) if the ratio of carbon-atom to fissile atoms stays constant then for two reactor systems with different voidage the carbon-atom displacement rate per unit nickel flux is constant within the errors of the calculation,

(b) if the heavy metal loading density in the fuel region is changed then for an homogeneous system the nickel flux fine structure across a cell stays the same,

(c) the effect of inserting an additional piece of graphite between the fuel and the moderator, and at the same time keeping the cell volume constant, is to decrease the nickel flux in the moderator but also to increase it in the fuel region.

4. REFERENCES

[1] R. Blackstone, Private Communication.

[2] D. L. Reed, "The Comparison of Carbon-Atom Displacement Rate in Graphite in the Dragon Reactor, the Petten HFR and a Low Enrichment HTR," D.P. Report 559.

[3] W. L. Zijp, et al., R.C.N. Internal Document.

[4] M. W. Thompson, S. B. Wright, "A New Damage Function for Predicting the Effect of Reactor Irradiation on Graphite in Different Neutron Spectra," AERE-R.4701.

[5] W. L. Zijp, et al., R.C.N. Internal Document.

[6] H. H. Yoshikawa, Private Communication.

[7] B. S. Gray and R. P. Thorne, "The Correlation of Graphite Irradiations," T.R.G. Report 1552 (C).

[8] J. C. Bell, et al., Phil. Trans. Roy. Soc. 254 361, 1962.

[9] H. Gutmann, B. Micheelsen and G. Preinreich, "Loading Calculations for the Dragon Reactor Experiment," D.P. Report 267.

[10] D. L. Reed and A. C. Bartlett, "The Relative Power Distribution and Integral Spectrum Measurements in the First Dragon Core," D.P. Report 442.

[11] H. Gutmann and H. Schober, Dragon Internal Document.

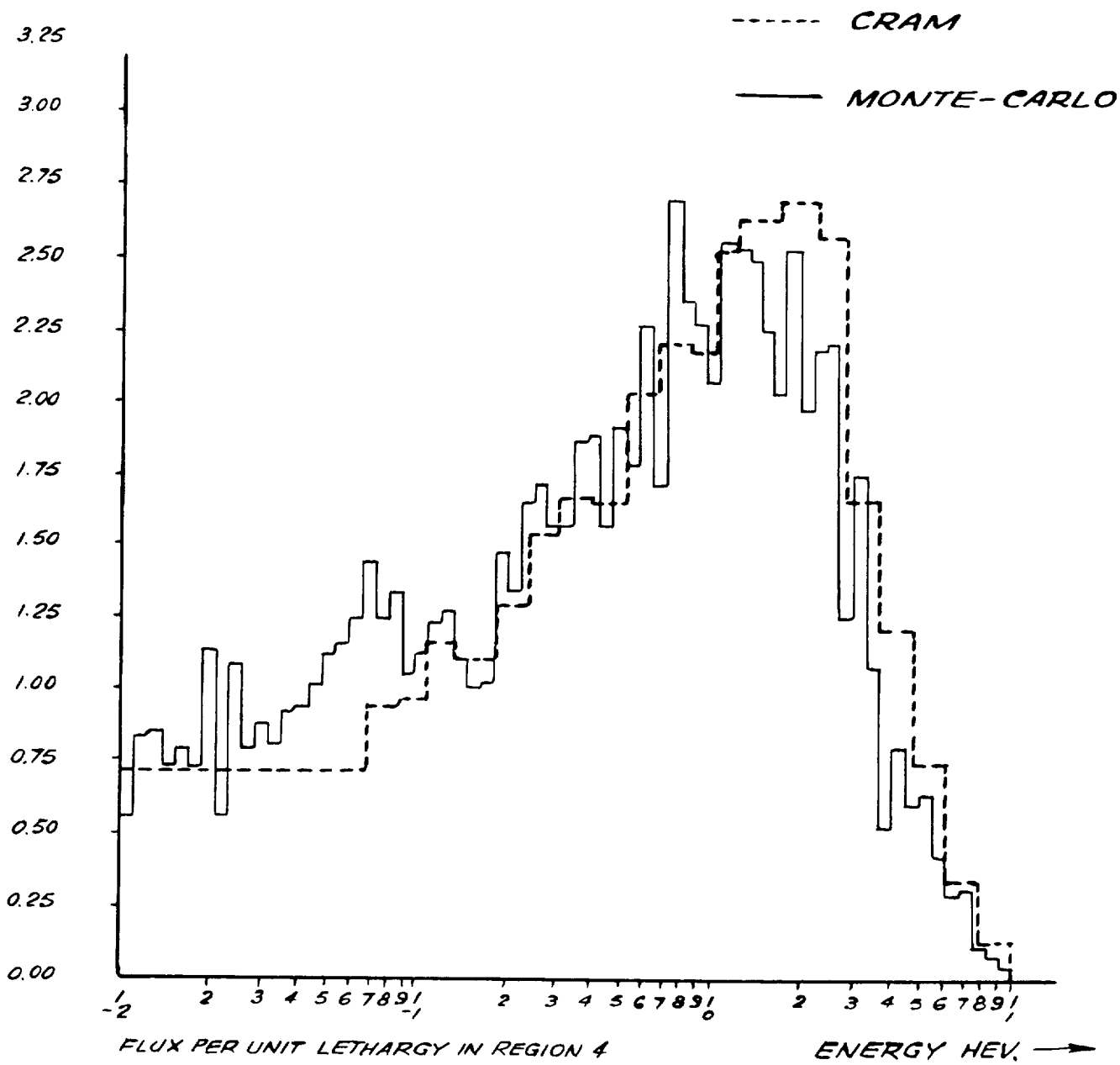

FIGURE 1.

NEUTRON SPECTRA IN THE DRAGON CAPSULE IN POSITION E8 IN PETTEN H.F.R.

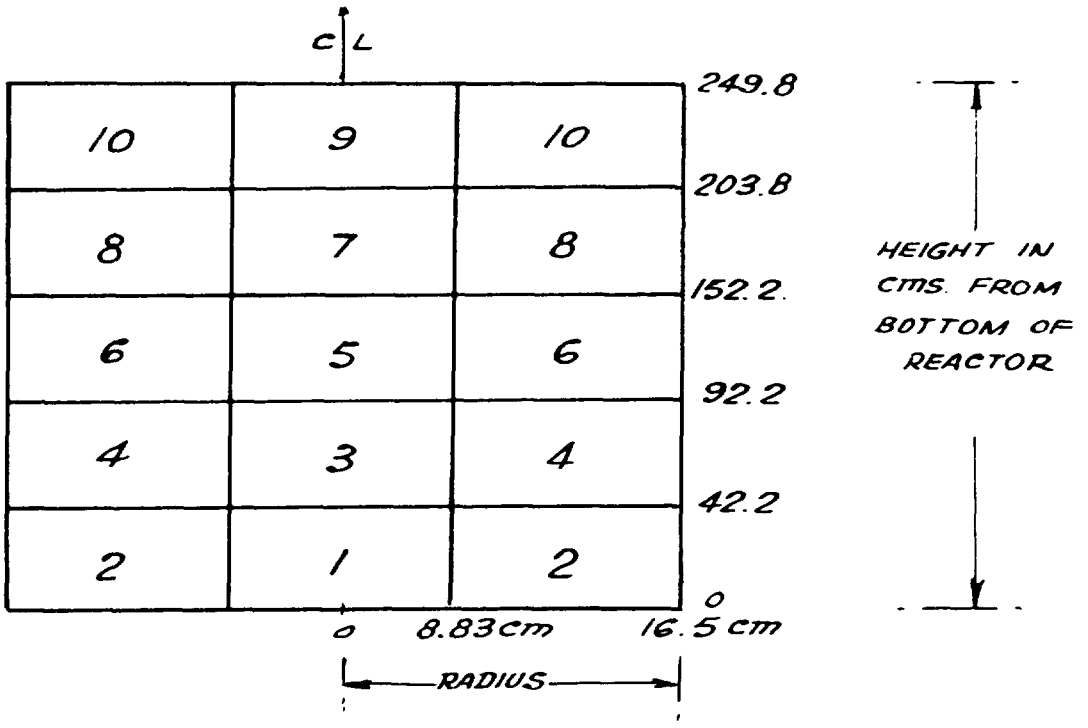

VERTICAL SECTION

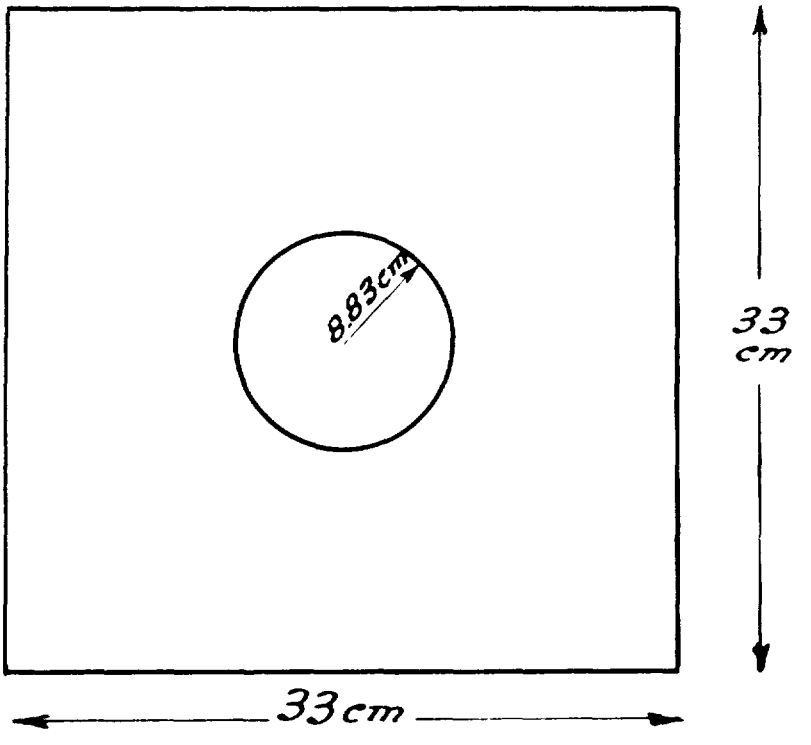

HORIZONTAL SECTION.

FIGURE 2. CASE 1.

SECTIONS THROUGH THE DRAGON REACTOR SHOWING REGIONS IN WHICH NEUTRON SPECTRA WERE CALCULATED.

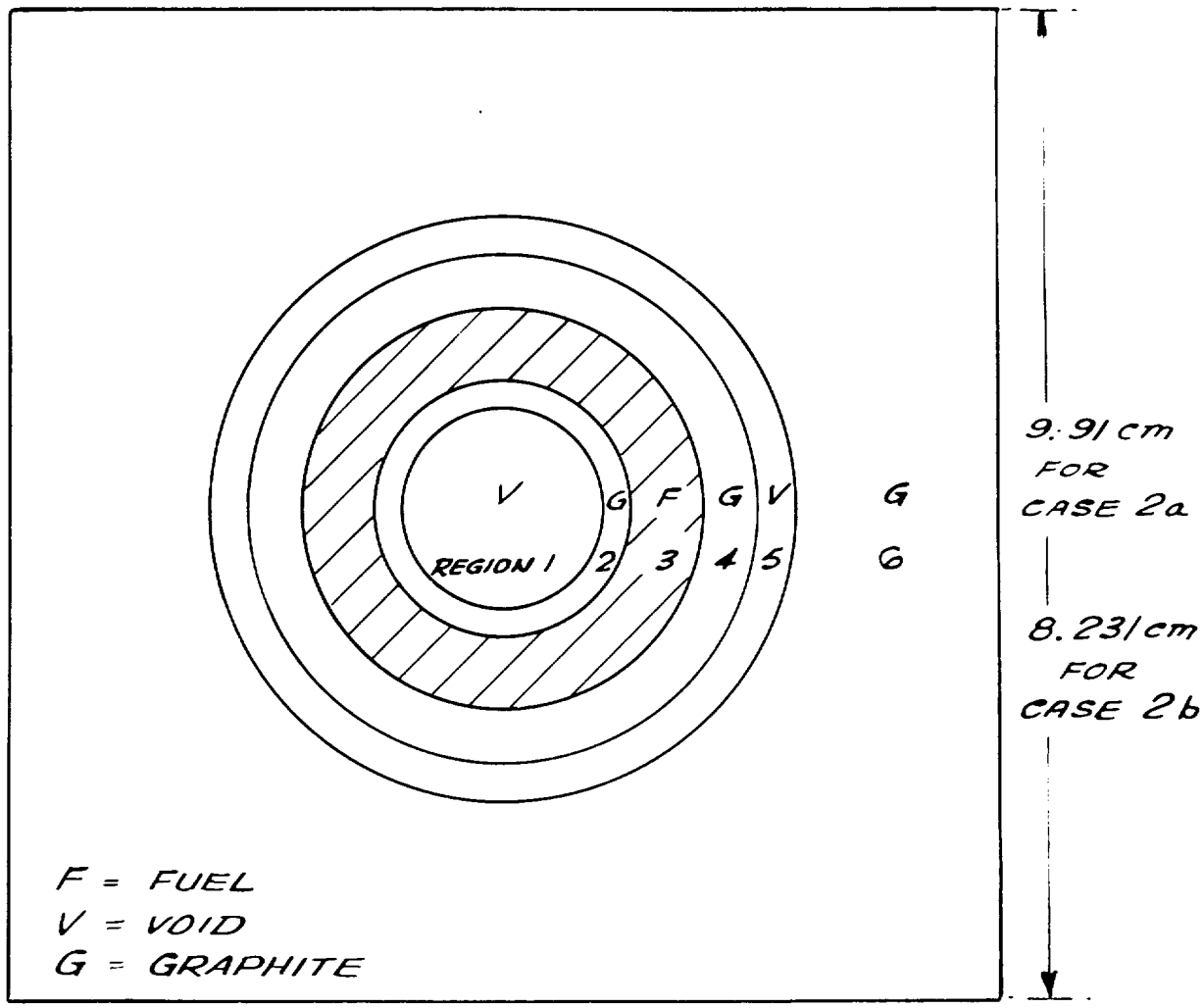

PLAN OF SLAB 1. AXIAL RANGE 0 TO 2.500E 01

FIGURE 3. CASES 2a AND 2b.
DIMENSIONS OF THE CELL OF HOMOGENEOUS H.T.R AND THE REGIONS FOR WHICH NEUTRON SPECTRA WERE CALCULATED.

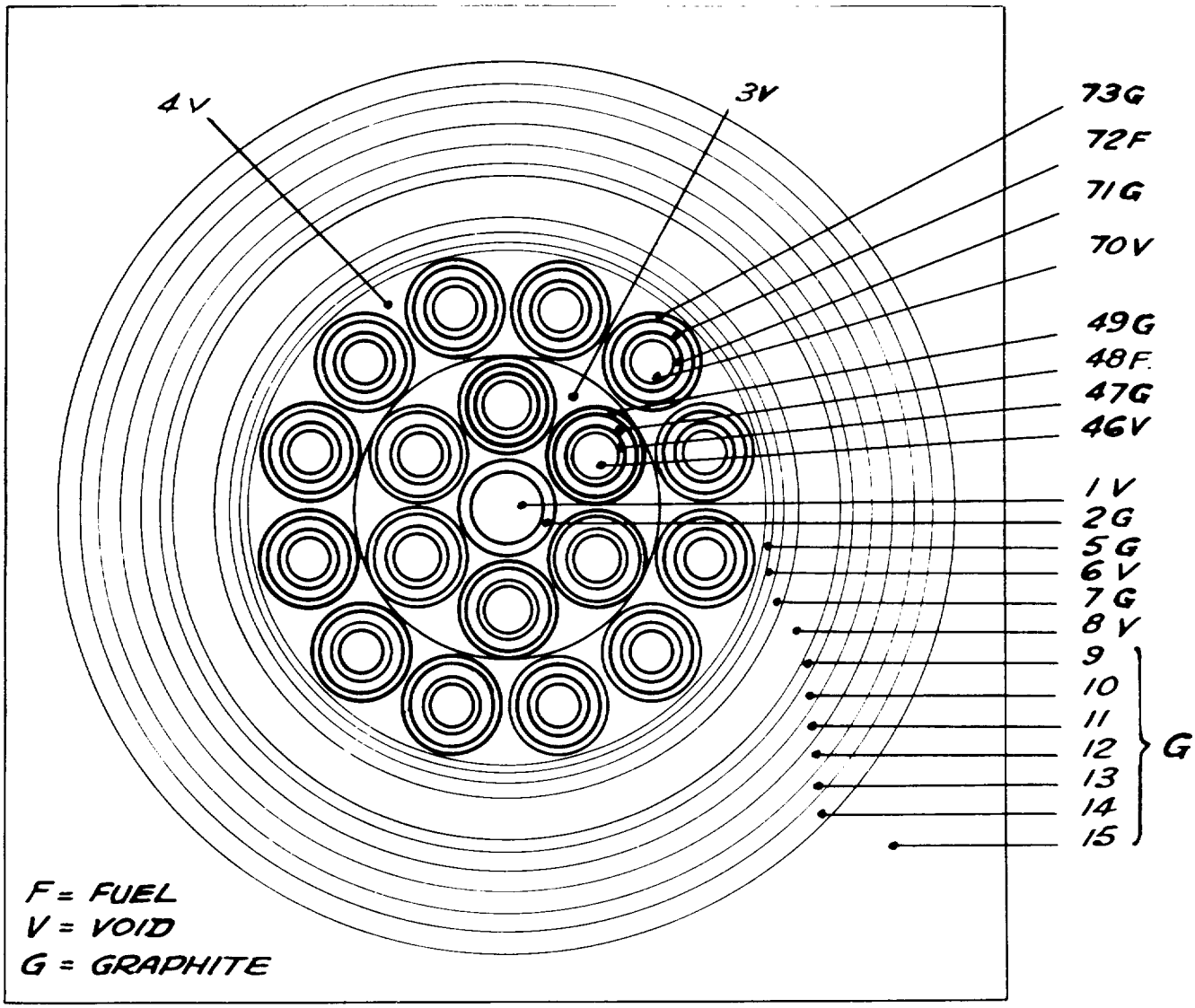

PLAN OF SLAB 1. AXIAL RANGE 0. TO 2.500E 01.

FIGURE 4. CASE 4.

REGIONS IN WHICH NEUTRON SPECTRA WERE CALCULATED FOR HETEROGENEOUS H.T.R WITH THE FUEL IN THE FORM OF A CLUSTER OF PINS.

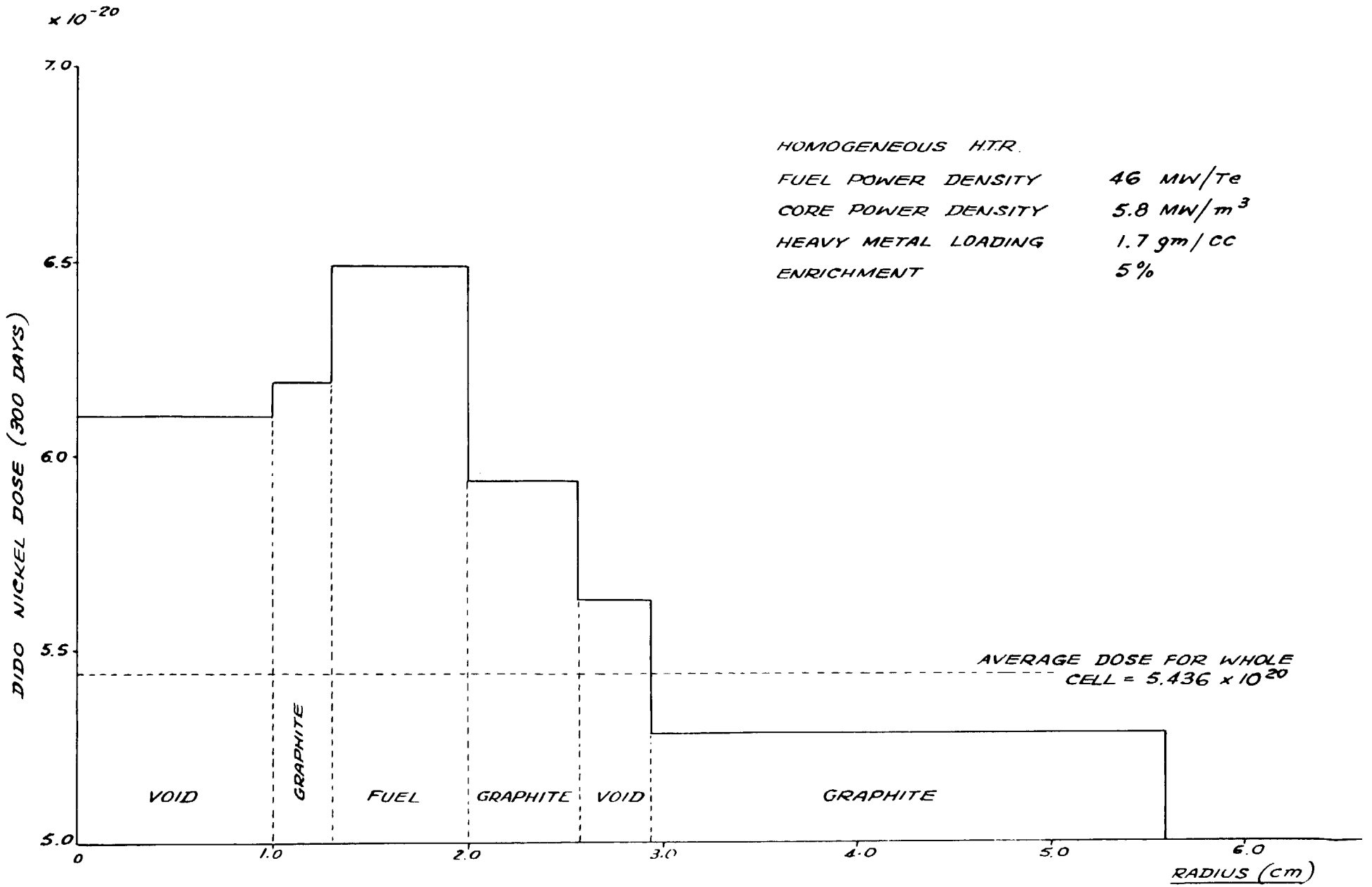

FIGURE 5 CASE 2a.

DIDO DOSE AFTER 300 DAYS VERSUS CELL RADIUS.

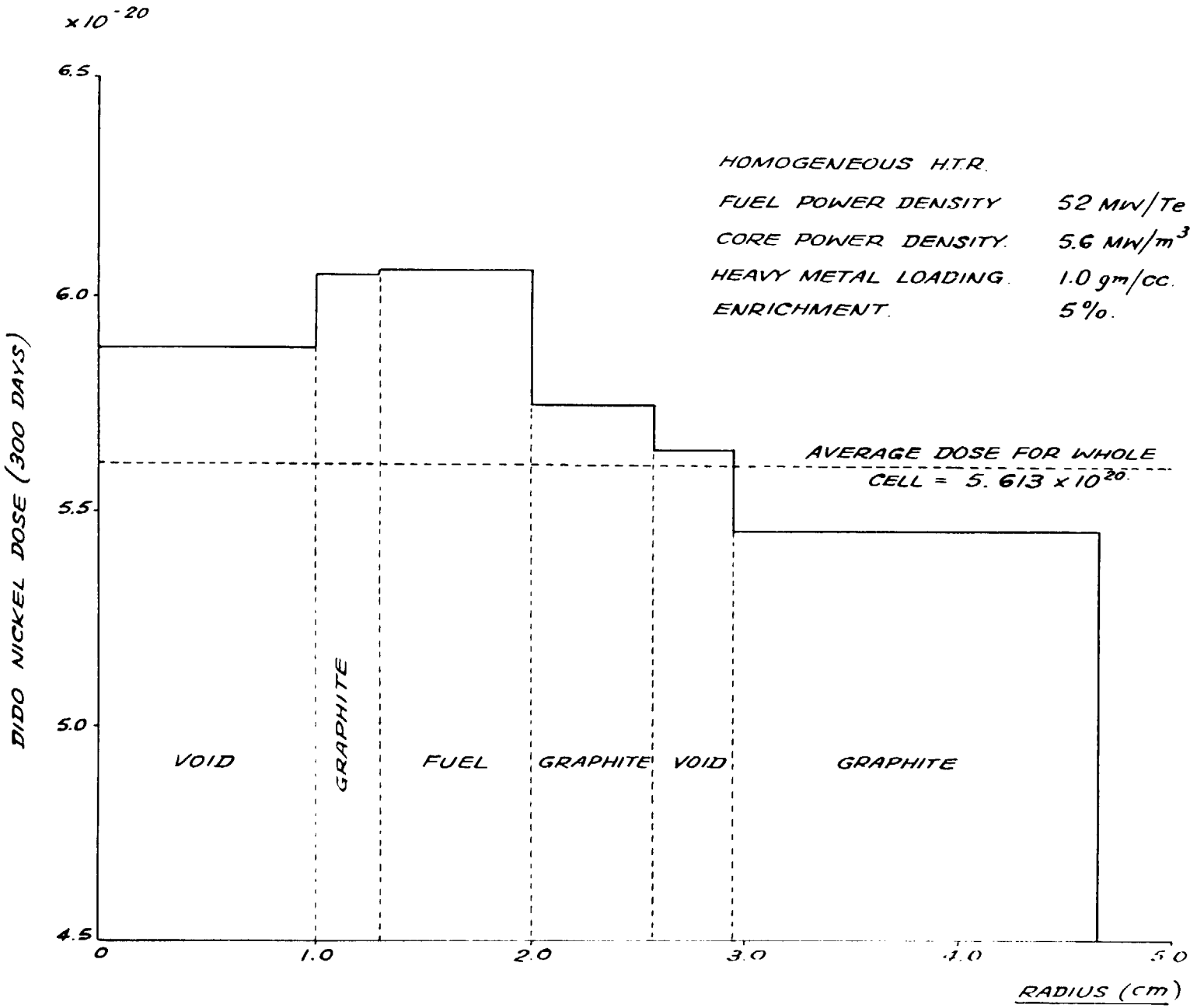

FIGURE 6. CASE 2b

DIDO DOSE AFTER 300 DAYS VERSUS CELL RADIUS

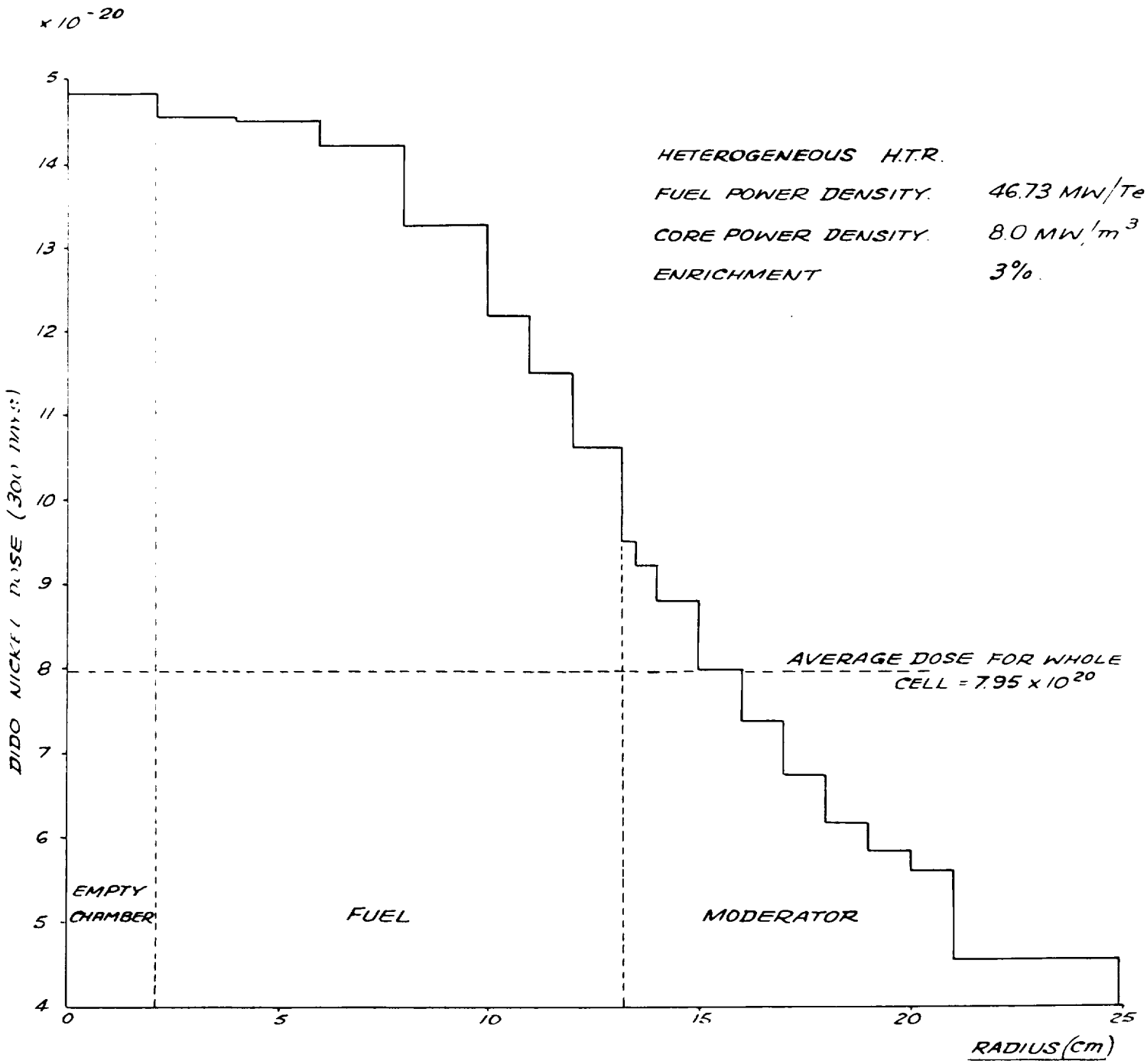

FIGURE 7. CASE 3.

DIDO DOSE AFTER 300 DAYS VERSUS CELL RADIUS.

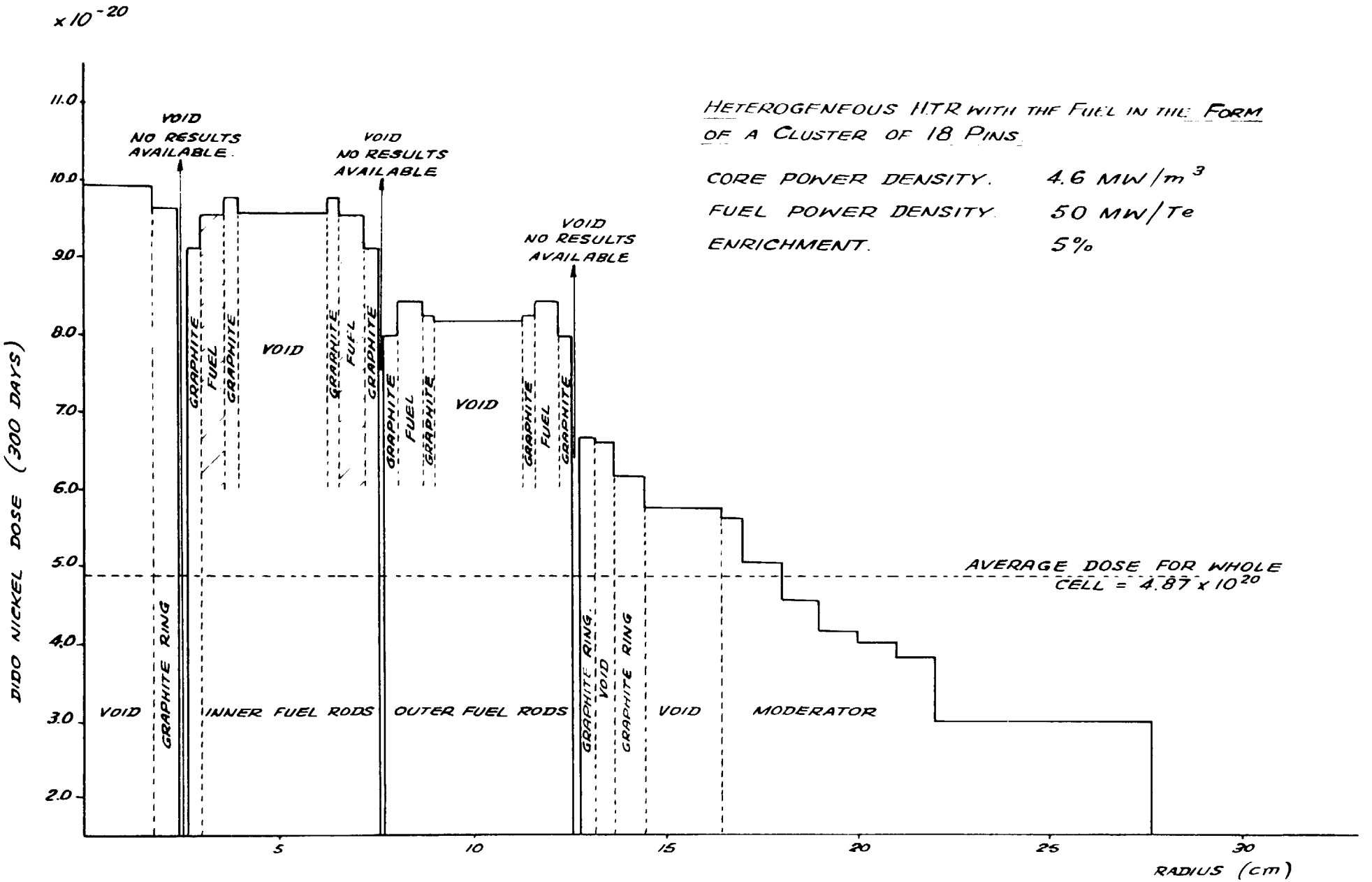

FIGURE 8. CASE 4

DIDO DOSE AFTER 300 DAYS VERSUS CELL RADIUS.

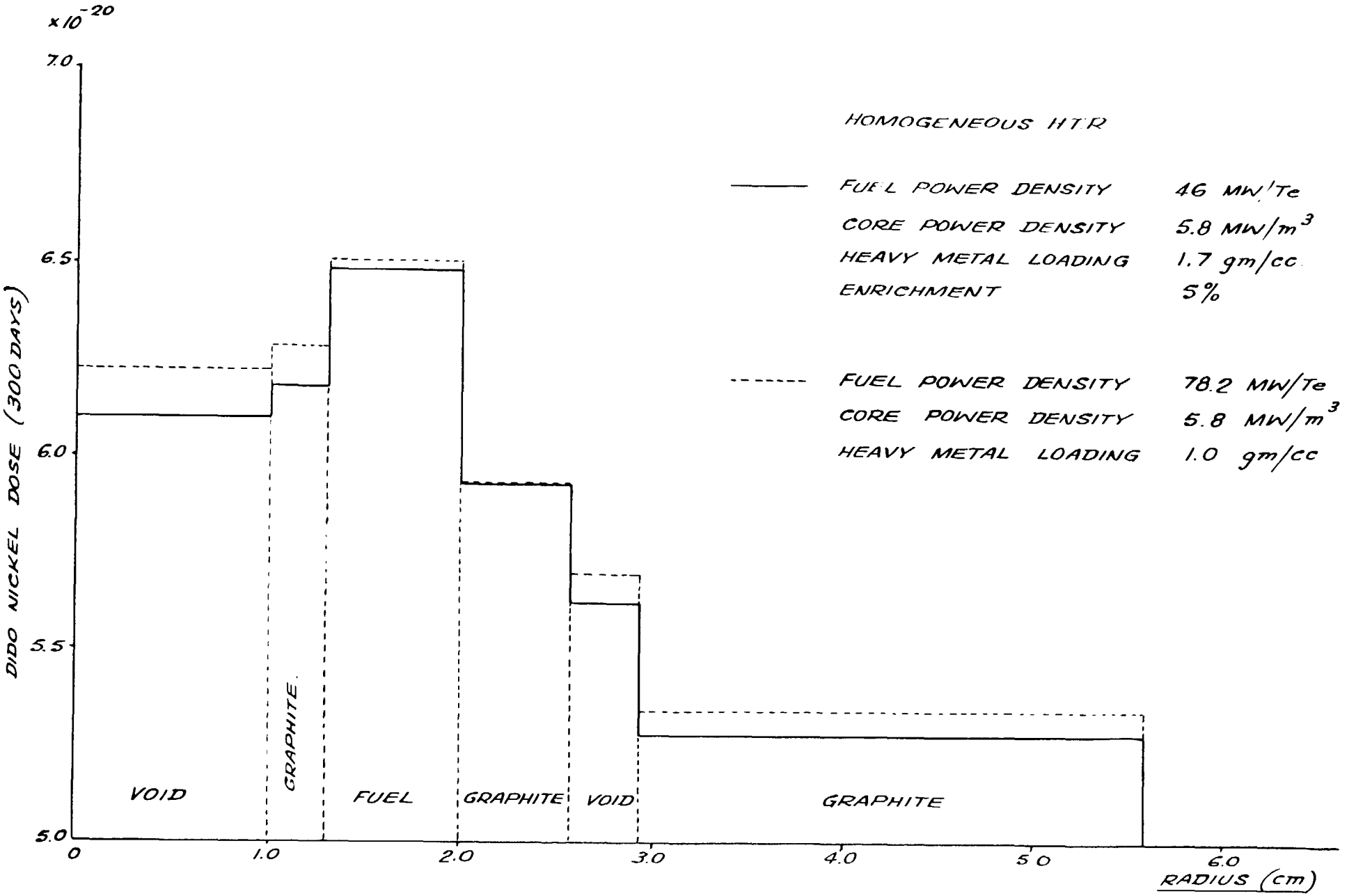

FIGURE 9.

COMPARISON OF THE DIDO DOSES AFTER 300 DAYS ACROSS A CELL FOR TWO DIFFERENT HEAVY METAL LOADINGS

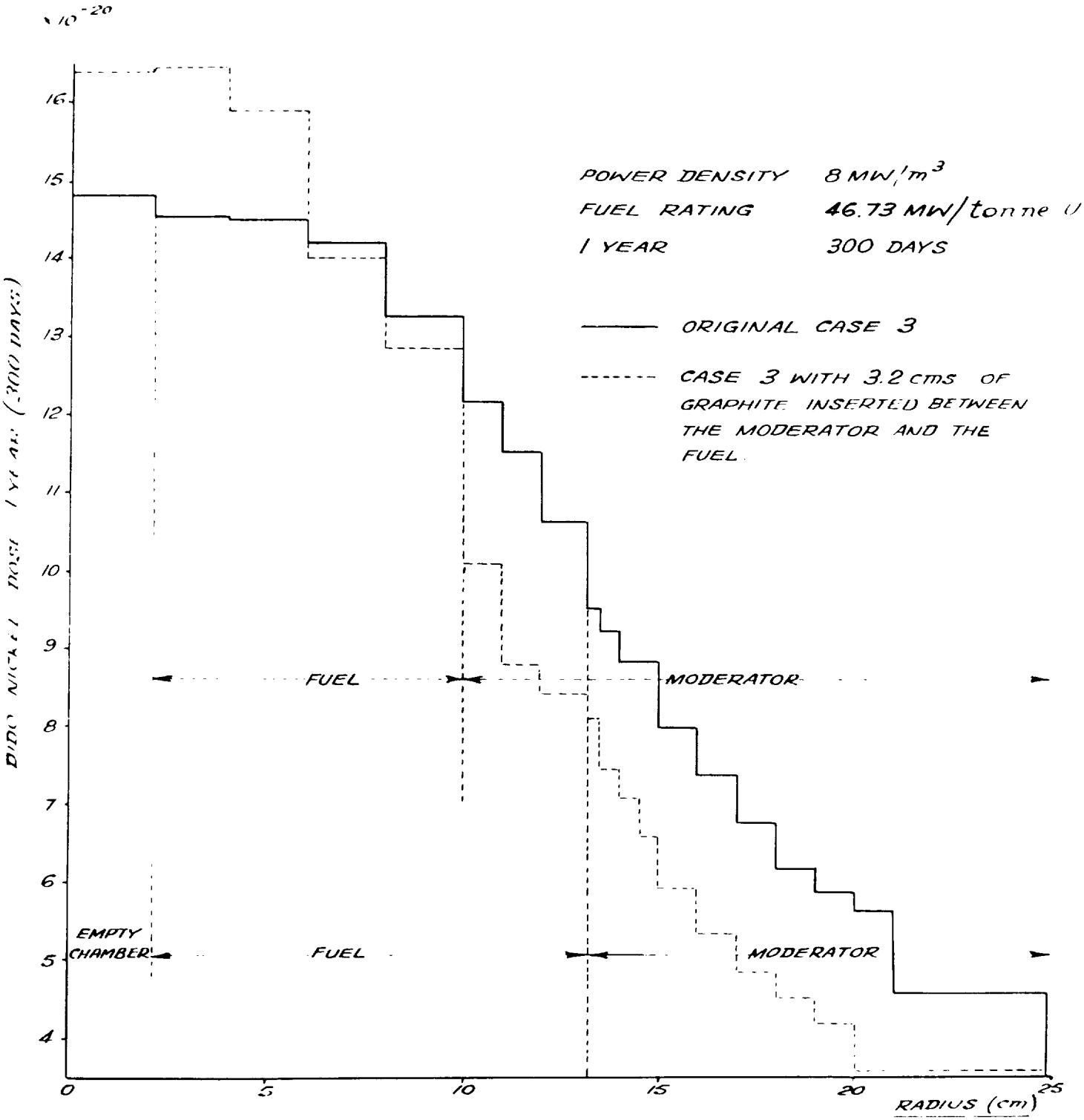

FIGURE 10

THE CHANGE OF DIDO NICKEL DOSE PROFILE IN A CELL OF A LOW ENRICHMENT H.T.R. WITH INCREASE IN SIZE OF MODERATOR REGION BUT KEEPING THE CELL VOLUME CONSTANT.

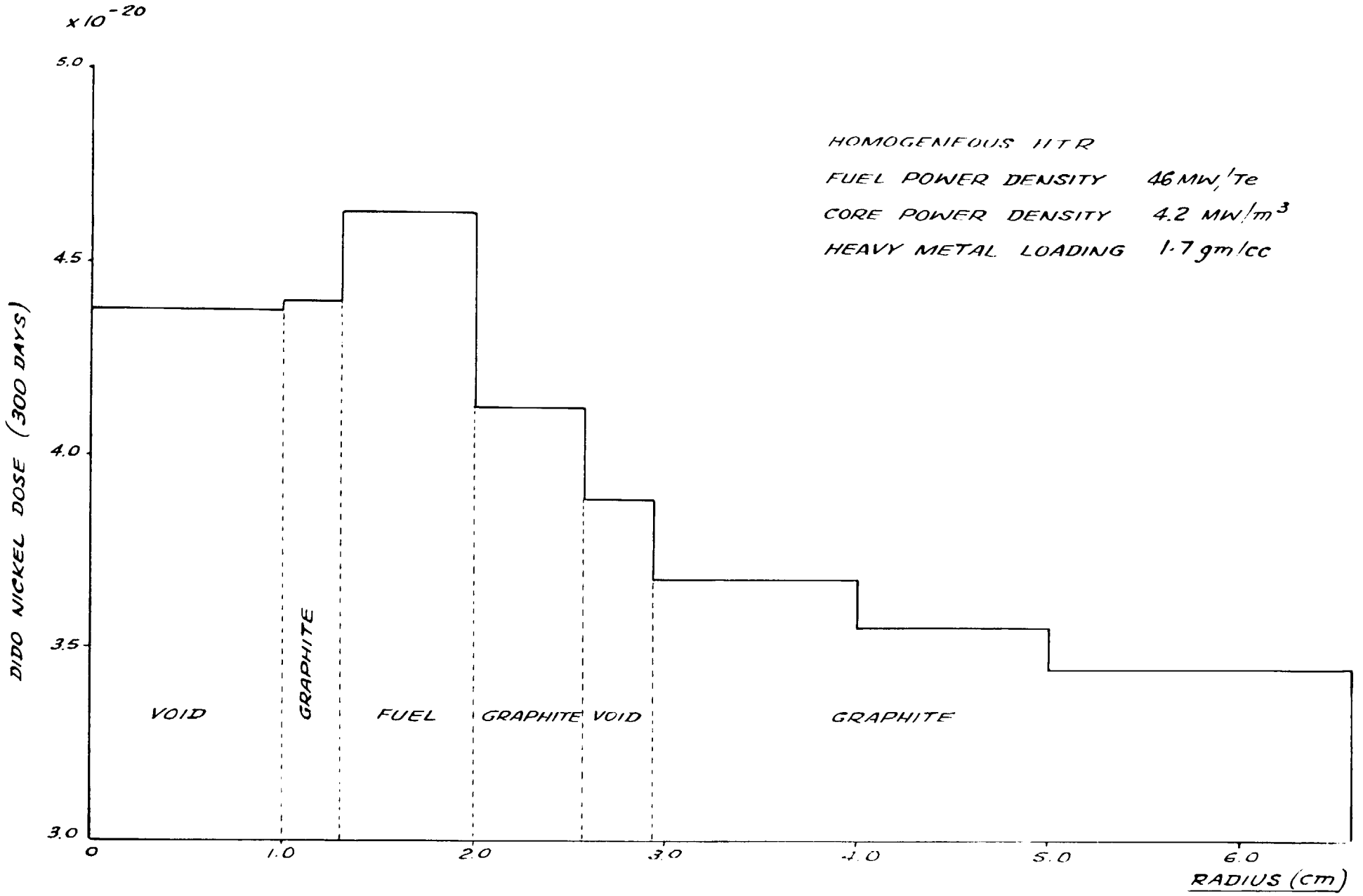

FIGURE 11 CASE 2a 1

DIDO NICKEL DOSE AFTER 300 DAYS VERSUS CELL RADIUS

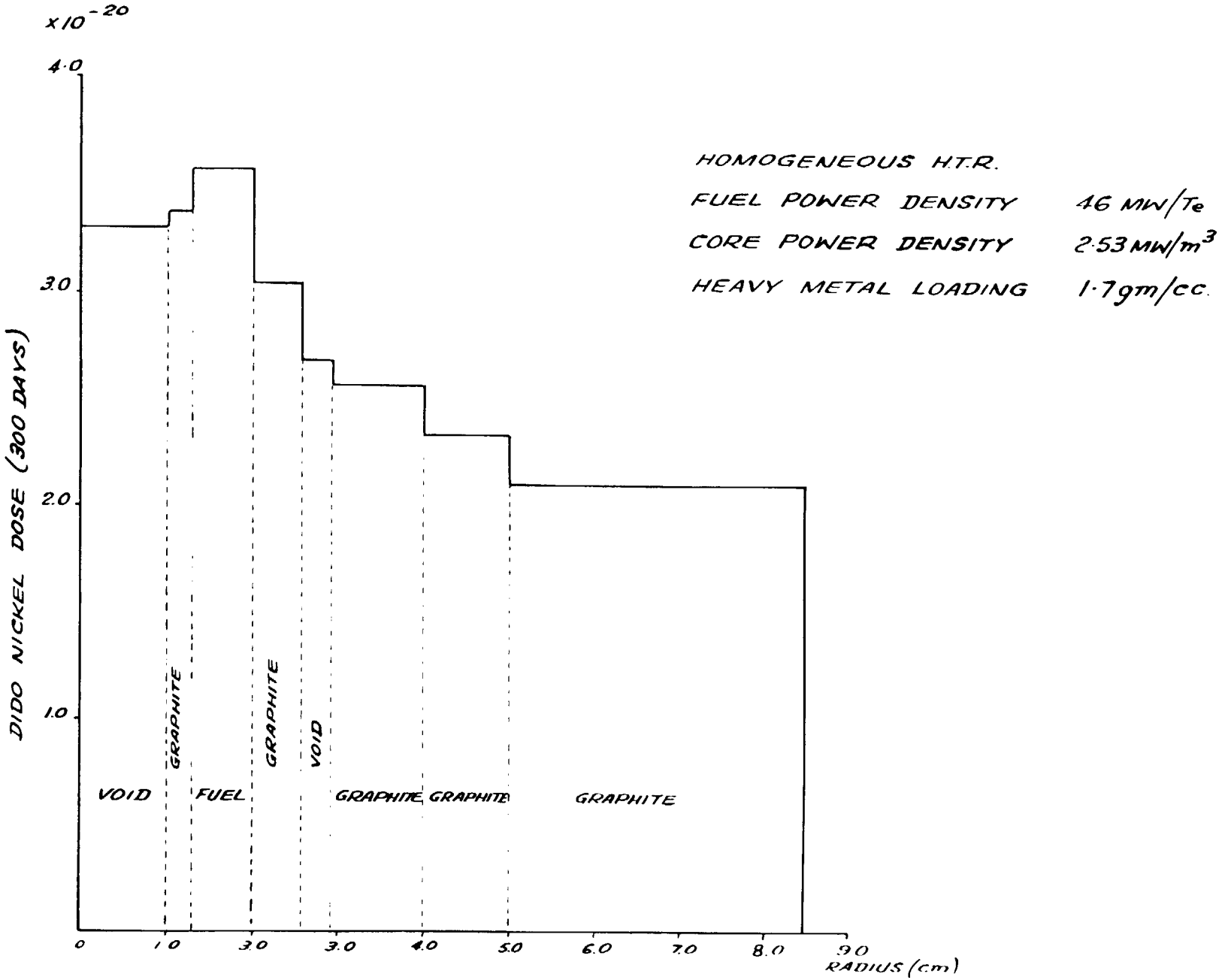

FIGURE 12

DIDO NICKEL DOSE AFTER 300 DAYS VERSUS CELL RADIUS